Critical thickness of the amorphous-nanocrystalline transition in Gd/Fe film structures

J. Landes, Ch. Sauer, B. Kabius, and W. Zinn
Institut für Festkörperforschung, Forschungszentrum Jülich, D-5170 Jülich, Germany
(Received 5 March 1991)

The growth of Gd/Fe layered structures prepared by evaporation in UHV was studied by means of *in situ* ^{57}Fe conversion-electron Mössbauer spectroscopy and cross-section high-resolution transmission electron microscopy. The Fe layer grows on the Gd sublayer in an amorphous structure up to a critical Fe thickness of $d_c = 2.3 \mp 0.1$ nm. On further increasing the Fe thickness, a rapid transformation to nanocrystalline structure throughout the total Fe layer occurs. This effect is suggested to be due mainly to the extreme misfit between the structural parameters of Fe and Gd.

Magnetic multilayer films composed by alternating layers of 3*d*-transition (*T*) and rare-earth (RE) metals have attracted considerable interest in recent years. This is mainly due to their magnetic properties comprising, e.g., perpendicular anisotropy (Fe/Nd, Fe/Dy)[1] or compensation point behavior (Fe/Gd)[2] for certain *T*-RE combinations. Those magnetic properties can be tailored by varying the relative thickness of the *T* and RE layers. For controlled film preparation it is important to study the detailed conditions of growth of such *T*/RE layered systems. Recently, a critical thickness $d_c = 2-2.5$ nm of the Fe layers in Fe/Dy (Ref. 3) and Fe/Y (Ref. 4) multilayer systems was observed. It was suggested that the Fe layers are amorphous for a Fe thickness below d_c and polycrystalline above d_c. According to the similar chemical and structural properties of the RE, the features of film growth should be quite similar for all combinations of Fe with RE crystallizing in the hcp structure.

We studied sandwich structures Gd/Fe/Gd as the simplest unit of a Fe/Gd multilayer sequence by means of ^{57}Fe conversion-electron Mössbauer spectroscopy (CEMS) and high-resolution transmission electron microscopy (HRTEM). CEMS is a sensitive microscopic method to analyze the magnetic [via the magnetic hyperfine (hf) field B_{hf}] and electronic properties (via the isomer shift) of the Fe layer. Furthermore, one can insert a thin probe layer consisting of a few monolayers (ML) of ^{57}Fe at a distinct position into the Fe layer, otherwise made of ^{56}Fe [no Mössbauer effect (ME) isotope]. In this way one can investigate the Fe film locally, e.g., at interfaces with a local resolution down to 1 ML.[5] In this paper we report on our results of the structural properties of Gd/Fe/Gd sandwich films.

Thin-film structures were prepared by evaporation in ultrahigh vacuum (UHV) on GaAs(110) and quartz glass substrates. Their composition was as follows: (substrate)/(10 nm Gd)/(d_{Fe} nm Fe)/(3 nm Gd)/(4 nm ^{56}Fe). The Fe interlayer of varying thickness d_{Fe} was made of the ME isotope ^{57}Fe. For analyzing the hf field profile across the Fe interlayer, ^{56}Fe was used with intercalating a 4-ML-thick ^{57}Fe probe layer at different positions within the ^{56}Fe layer. For evaporation of the Fe isotopes and of the Gd small Al_2O_3 crucibles and an electron-beam-heated W crucible were used, respectively. The base pressure of the preparation chamber amounted to 3×10^{-8} Pa. During evaporation the pressure was about 1×10^{-7} Pa and the partial pressures of oxygen and hydrogen (critical gases for RE) were about 2×10^{-9} Pa and 1×10^{-8} Pa, respectively. The evaporation rate was 0.1 Å/s, and the substrate temperature was varied from -50 °C to 250 °C. Film thickness (accuracy $\approx$ 5%) was controlled using a quartz oscillator for each crucible. Quartz calibration could be checked by moving another quartz at the substrate position. As judged from ME spectra the samples were stable during a storage time of several months in dry air.

In situ CEMS experiments were performed in an UHV system combining a preparation and CEMS chamber.[6,7] The ME source was (^{57}Co)Rh. For HRTEM a JEOL 4000-EX microscope running at 400 KV was used. The cross-section samples were prepared by 5-keV argon-ion milling.

All ME spectra measured at 300 K could be decomposed into three subspectra of the characteristic shape labeled by *P*, *A*, and *B* as shown in Fig. 1. The relative contributions of these subspectra depend on the thickness d_{Fe} of the Fe interlayer. Subspectrum *P* is a broadened doublet with a quadrupole splitting of $\approx$0.25 mm/s, which does not split magnetically down to 90 K. Subspectrum *A* looks like a Fe spectrum of an amorphous magnetic material, with a distribution of hf fields B_{hf} around a mean value of $\bar{B}_{hf} \approx 21$ T (at 300 K) for the samples with $d_{Fe} > 0.8$ nm. In the region $0.4 \le d_{Fe} < 0.8$ nm, $\bar{B}_{hf}$ increases from 0 to 21 T. In contrast, the subspectrum *B* reveals the typical six-line pattern of bcc α-iron with broadened line widths. The hf fields of spectrum *B* are slightly reduced as compared to the Fe bulk value of B_{hf}(bulk) = 33.3 T (300 K). They increase to $B_{hf} = 31-32.7$ T with increasing d_{Fe}. While spectrum *B* shows also the right isomer shift of $S = -0.1$ mm/s of bcc Fe [referred to (^{57}Co)Rh], the spectra of types *A* and *P* are shifted to $S = -(0.15-0.18)$ mm/s, implying an enhanced *s* electron density at the ^{57}Fe nucleus.

The contributions of the three subspectra are plotted in Fig. 2 versus the total thickness d_{Fe} of the Fe interlayer. Instead of the relative fraction *R* as obtained from the relative area of the subspectra, we plotted their partial thicknesses $d_i = R_i d_{Fe}$ ($i = P, A, B$). Type *P* remains con-

stant with increasing d_{Fe} at the value $d_P \approx 0.4$ nm (≈ 2 Fe ML). At $d_{Fe} \approx 0.4$ nm, type A appears, and its contribution increases roughly linearly with d_{Fe}. This changes sharply at $d_{Fe} = (2.3 \mp 0.1)$ nm, where type B suddenly grows up at the expense of type A.

On raising the substrate temperature in the range $T_s = 10\,°C - 170\,°C$, the data given in Fig. 2 hardly change, i.e., the critical thickness $d_c = 2.3$ nm and the relative contributions remain nearly constant. Only the amount of type P increases weakly with T_s at the expense of type A. Hence, spectrum P may be related to interdiffusion at the Fe/Gd interface, which is also consistent with its isomer shift and doublet shape.[8] However, the range of such a intermixing should be restricted to 1–2 ML as we will point out later. On lowering T_s to $-50\,°C$, d_c increases slightly to 2.6 nm and the contribution of type A increases at the expense of type B. This can be explained by reduced surface mobility of the Fe atoms during evaporation, resulting in an increase of lattice defects. The optimum value was found to be $T_s = 0\,°C - 100\,°C$.

The results support the suggestion of a critical Fe thickness for the transformation from amorphous (A) to polycrystalline (B) Fe film structure.[3,4] According to Fig. 2 this transition is very sharp in Gd/Fe systems. In principle, the shape of the type A spectra could also be caused by an amorphous Fe/Gd alloy, i.e., by a solid solution of Fe in Gd. However, in a layered system where Fe and Gd were evaporated alternately this would presuppose a strong interdiffusion and solubility, which is very unlikely according to the Fe-Gd phase diagram and the small solubility of <0.6 at. % Fe in Gd.[9] Also, assuming a Gd-Fe solution one must suppose that on crossing the critical crystallization thickness Fe and Gd will segregate into flat layers, because the HRTEM images (discussed below) give no indication of clustering. This is not quite reasonable. Furthermore, the possible existence of amorphous intermetallic compounds like $GdFe_2$ is improbable. All such Gd-Fe compounds reveal saturation hf fields[10] of $B_{hf} \approx 21-23$ T, compared to the low-temperature values of our type A films ($d_{Fe} < d_c$) of $\bar{B}_{hf} \approx 30$ T. Also, they must decompose then at d_c, which is quite unlikely. As a consequence, the shape of our type A spectra can be explained by pure amorphous Fe but not by an alloylike Fe-Gd mixing.

Using the aforementioned ^{57}Fe probe layer technique we measured the ME spectra locally at the bottom (Gd/Fe interface near substrate), the center, and top of the Fe interlayer in a (10 nm Gd)/(d_{Fe} ^{56}Fe)/(3 nm Gd)/(5 nm Al) film structure ($d_{Fe} = 2.2$, 2.9, 4.1 nm). The ^{57}Fe probe layer was 3–4 ML ^{57}Fe thick. Figure 3 shows the spectra of $d_{Fe} = 4.1$ nm samples. Apparently, the bulklike subspectrum of type B is dominating in the center [Fig. 3(b)] beside a small amount of type A. In contrast, at both Fe/Gd interfaces [Figs. 3(a) and 3(c)] type B is still present, but here type P and A contribute largely. Obviously the disturbed Fe regions are restricted to interface zones of 2–3 ML thickness, while the center is crystallized. There seems to be no significant difference between the bottom and the top interfaces. Samples with $d_{Fe} = 2.2$ nm $< d_c$ exhibit only the spectra of type A and P, where type P is found in the interface regions only. The total amount of the spectrum P corresponds to a par-

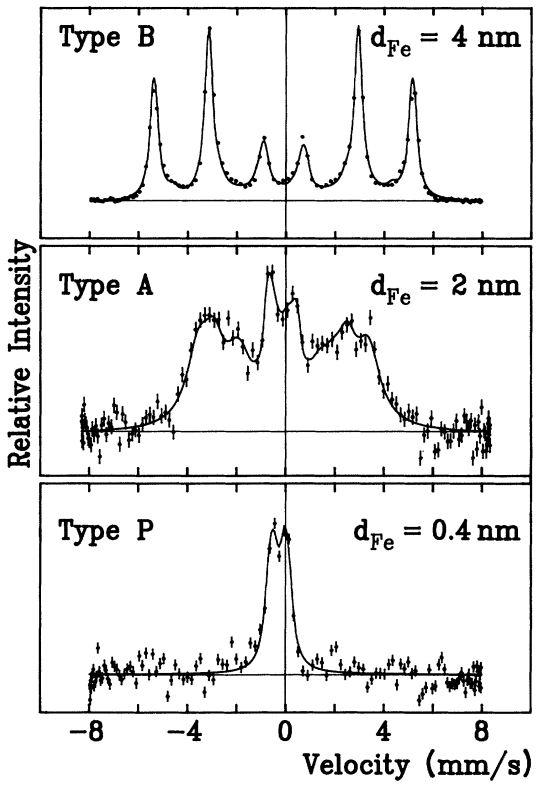

FIG. 1. ME spectra of Gd/(d_{Fe} ^{57}Fe)/Gd films ($d_{Fe} = 0.4$, 2.0, 4.0 nm) at 300 K representing the characteristic subspectra labeled by P, A, and B (see text).

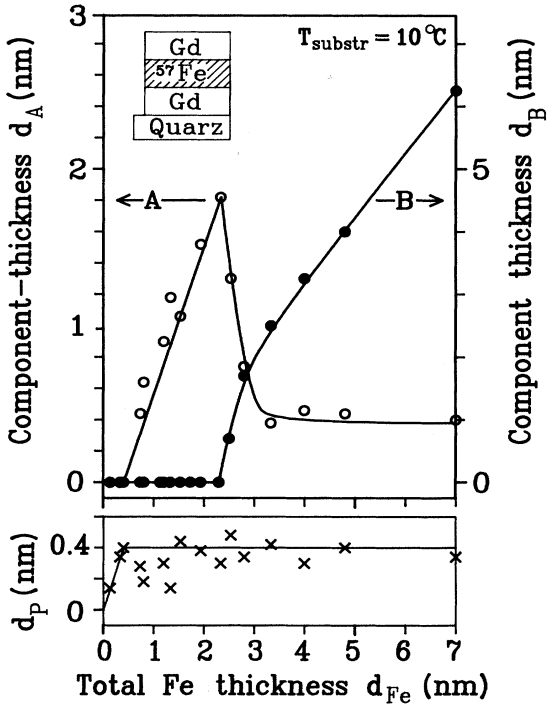

FIG. 2. Partial thicknesses d_P, d_A, d_B of the different contributions to the ME spectra vs total Fe thickness d_{Fe} (see text).

tial thickness of $d_P \approx 0.4$ nm ≈ 2 Fe ML (Fig. 2). Thus, those paramagnetic Fe atoms should be concentrated mainly within the first ML at both interfaces.

We conclude that the suggestion of Refs. 3 and 4 also holds for the Fe/Gd system: the Fe interlayer crystallized at a critical Fe thickness of $d_c = 2.3$ nm. The ME spectrum of type A can be attributed to amorphous pure metallic Fe and type B to nanocrystalline Fe. Further evidence for this interpretation comes from HRTEM images of cross sections of two samples with $d_{Fe} = 1.6$ nm $< d_c$ [Fig. 4(a)] and $d_{Fe} = 3.2$ nm $> d_c$ [Fig. 4(b)]. The GaAs(110) substrates provide a calibrated length scale. According to the ME spectra there was no difference between films prepared on quartz glass and GaAs substrates.

The HRTEM analysis yielded the following results: Gd grows directly on GaAs(110) with amorphous structure. At about 4.5 nm thickness the Gd film starts to become nanocrystalline (grain size 3–5 nm) with hcp structure, while the first 4.5 nm still remain amorphous. The Gd grains grow preferentially with the c axis oriented nearly perpendicular to the film plane. The lattice parameter c is enlarged up to 4% in some Gd grains. On top of the 10-nm Gd film, in fact, the Fe layer is amorphous in the samples with $d_{Fe} = 1.6$ nm [Fig. 4(a)]. Unfortunately, the Fe and the subsequently grown 3-nm Gd film can hardly be distinguished, because both are amorphous, and the diffraction and absorption contrast is not sufficiently high. However, in the sample with $d_{Fe} = 3.2$ nm [Fig. 4(b)], the first Gd film (10 nm) is identical, while the following Fe film clearly grows nanocrystalline with grain sizes of 1–3 nm perpendicularly and up to 7 nm for in-plane direction. The lattice distance as obtained from the image [Fig. 4(b)] is in close accordance with bcc bulk Fe ($a = 0.286$ nm), showing deviations of -5% to $+3\%$ for some grains. Obviously, the HRTEM analysis agrees with the CEMS study, suggesting amorphous structure of the Fe interlayer for $d_{Fe} < d_c$ and nanocrystalline structure for $d_{Fe} > d_c$.

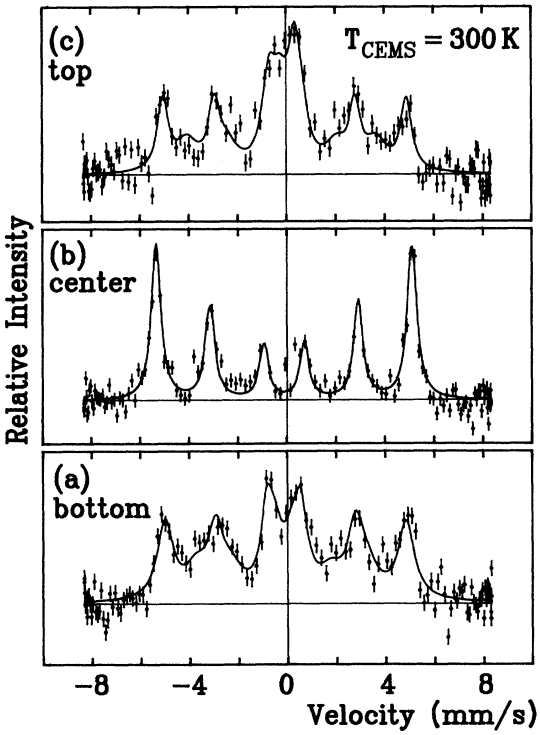

FIG. 3. ME spectra of center part and Gd/Fe interface regions (bottom, top) in a (quartz glass)/(10 nm Gd)/(4.1 nm ^{56}Fe)/(3 nm Gd) film at 300 K as measured by the ^{57}Fe probe layer technique.

The bulklike spectrum of type B must be attributed to the nanocrystalline phase. From the volume dependences of isomer shift $dS/d\ln V = 1.38$ mm/s (Ref. 11) and hf field $d\ln B_{hf}/d\ln V = 0.372$,[12] one can estimate that the observed scattering in lattice parameters of the Fe grains causes a spread of $\Delta S = +0.1$ mm/s and $\Delta B_{hf} = +1.1$ T. This can explain the line broadening observed in the type B spectra. Certainly, the aforementioned reduction of the hf fields of type B spectra (31–32.7 T) will be related to the average Fe grain size. But a further explanation may be that the Fe hf field at the Fe/Gd interface is strongly reduced[13] similarly to the Fe/Cr interface.[5] While the Fe-Cr interaction is of short range (≈ 3 ML) the influence of Fe/Gd interface extends up to 3 nm into the Fe film.[13] Thus, even a 6-nm-thick Fe interlayer can hardly obtain the full bulk hf field.

Now the question arises whether the amorphous phase of the Fe interlayer is due to intercalation between two Gd films or only to the lattice mismatch between Fe and the preceding Gd film. We prepared films of the structure (quartz glass)/(7 nm Gd)/(d_{Fe} ^{57}Fe) with $d_{Fe} = 2.0, 2.3, 2.6, 3.6$ nm (without cover) at $T_S = 10$ °C. Immediately after preparation, CEMS spectra were measured *in situ* in time intervals of 30 min. As a result, we found exactly the crystallization behavior of the intercalation case and no time dependence. Consequently, the crystallization process must take place during, or at least within 2 min after finishing the Fe deposition, which follows from the evaporation procedure. It should also be noted that a stepwise annealing of a Gd/Fe double layer with $d_{Fe} = 2.3$ nm at 250 °C and 350 °C increases the bulklike at the expense of the still present amorphous phase.

These results indicate that the amorphous growth of the Fe layer is not a multilayer effect but is caused rather by the interplay at the Gd/Fe interface. Fe and Gd show large differences with respect to atomic radius (0.126 or 0.179 nm), crystal structure (bcc or hcp), lattice parameters ($a = 0.286$ nm or $a = 0.362$ nm, $c = 0.575$ nm), electronegativity (1.8 or 1.1) and surface energy (2.55, ≈ 0.9 J cm^{-2}).[14] For Fe/Mg multilayer systems (hcp Mg) the data also differ strongly, but less so compared to Fe/RE (hcp) systems. In fact, there seems to exist in Fe/Mg systems some kind of a critical thickness amounting to about 1.2 nm, which is derived from ME spectra and magnetic properties.[15] Hence, we suppose that essentially the structural misfit between the Fe and RE layers is responsible for the amorphous growth mode of the Fe layers. In the usual theories of recrystallization (e.g., Ref. 16), which is a similar process, a critical size of nuclei of 0.1–1 μm is necessary to start the recrystallization. This

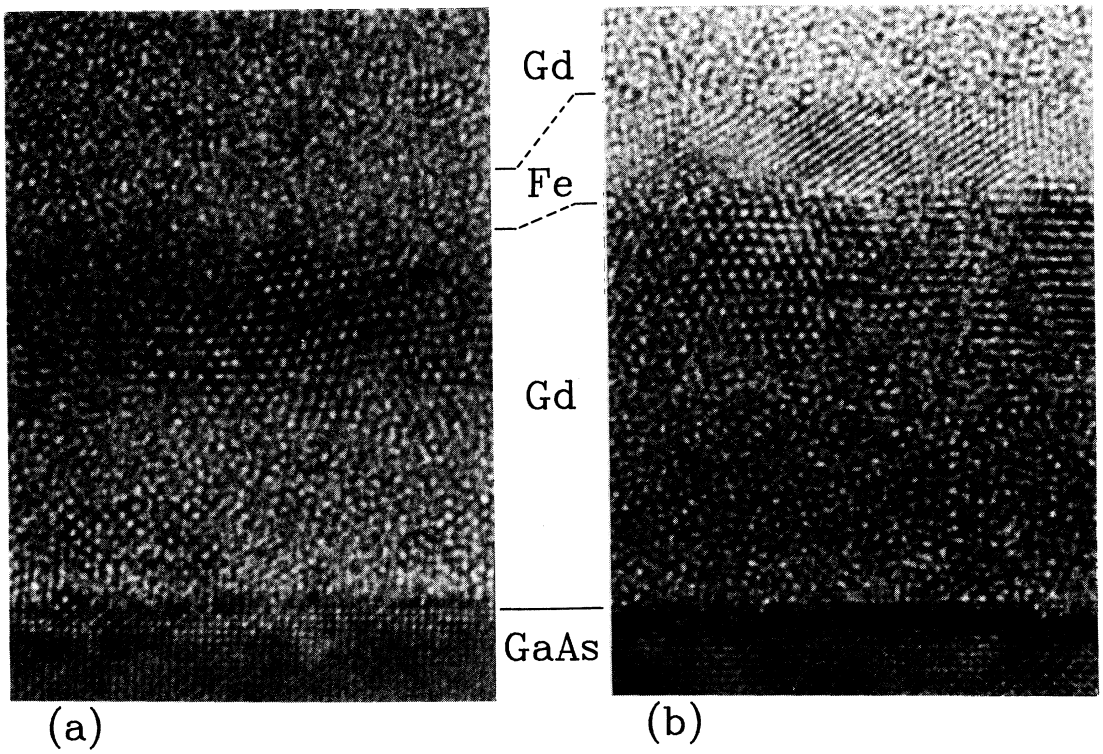

FIG. 4. Cross-section HRTEM images of two GaAs(110)/(10 nm Gd)/Fe/(3 nm Gd)/(10 nm Al) films with thicknesses d_{Fe} of 1.6 nm (a) and 3.2 nm (b). In (b) the Fe interlayer is nanocrystalline.

size is determined by the competition between the surface tension of the grains and stored energy due to lattice distortions. To our knowledge, however, a theory for crystallization on an atomic scale, i.e., in the nm region, is not yet available.

In conclusion, in Gd/Fe layered systems the Fe layers grow first in an amorphous structure on the Gd layer, up to a critical thickness of $d_c = 2.3$ nm. By further increasing the Fe thickness a transformation into nanocrystalline structure throughout nearly the whole Fe layer is observed. We suppose that this effect will occur in all Fe/RE film systems, where the pure RE film would crystallize in hcp structure. This growth mode seems to be due to the extreme misfit between bcc Fe and hcp RE. Those systems may also offer an opportunity to study the magnetic properties of amorphous metallic Fe, which were so far extrapolated[17] only from amorphous $Fe_{1-x}M_x$ alloys (the RE M = Gd, Tb, Dy, or Ho) to $x = 0$. An investigation of the Fe/Y film system (without the disturbing magnetism of Gd) is in progress.[18]

[1]N. Hosoito, K. Yoden, K. Mibu, and T. Shinjo, J. Phys. (Paris) Colloq. **49**, C8-1777 (1988).
[2]Y. Kamiguchi, Y. Hayakawa, and H. Fujimori, Appl. Phys. Lett. **55**, 1918 (1989).
[3]K. Yoden, N. Hosoito, K. Kawaguchi, K. Mibu, and T. Shinjo, Jpn. J. Appl. Phys. **27**, 1680 (1988).
[4]T. Morishita, Y. Togami, and K. Tsushima, in *Proceedings of the International Symposium on Physics of Magnetic Materials, Sendai, 1987,* edited by M. Takahashi, S. Maekawa, Y. Gondo, and H. Nose (World Scientific, Singapore, 1987), p. 295.
[5]J. Landes, Ch. Sauer, R. A. Brand, W. Zinn, S. Mantl, and Zs. Kajcsos, J. Magn. Magn. Mater. **86**, 71 (1990).
[6]Ch. Sauer, A. Holzwarth, Zs. Kajcsos, and W. Zinn, Nucl. Instrum. Methods B **34**, 377 (1988).
[7]Zs. Kajcsos, Ch. Sauer, A. Holzwarth, R. Kurz, W. Zinn, M. A. C. Ligtenberg, and G. van Aller, Nucl. Instrum. Methods B **34**, 383 (1988).
[8]M. Forker, R. Trzcinski, and T. Merzhäuser, Hyperfine Interact. **15-16**, 273 (1983).
[9]O. Kubaschewski, *Iron Binary Phase Diagrams* (Springer, Berlin, 1982).
[10]U. Atzmony and M. P. Dariel, Phys. Rev. B **10**, 2060 (1974).
[11]A. J. Moyzis, Jr. and H. G. Drickamer, Phys. Rev. **171**, 389 (1968).
[12]D. L. Williamson, S. Bukshpan, and R. Ingalls, Phys. Rev. B **6**, 4194 (1972).
[13]J. Landes, Ch. Sauer, and W. Zinn (unpublished).
[14]A. R. Miedema and J. W. F. Dorleijn, Surf. Sci. **95**, 447 (1980).
[15]K. Kawaguchi, R. Yamamoto, N. Hosoito, T. Shinjo, and T. Takada, J. Phys. Soc. Jpn. **55**, 2375 (1986).
[16]J. D. Verhoeven, *Fundamentals of Physical Metallurgy* (Wiley, New York, 1975).
[17]N. Heiman, K. Lee, and R. I. Potter, J. Appl. Phys. **47**, 2634 (1976).
[18]J. Landes, S. Dörrer, U. Köbler, A. Fuss, Ch. Sauer, and W. Zinn (unpublished).

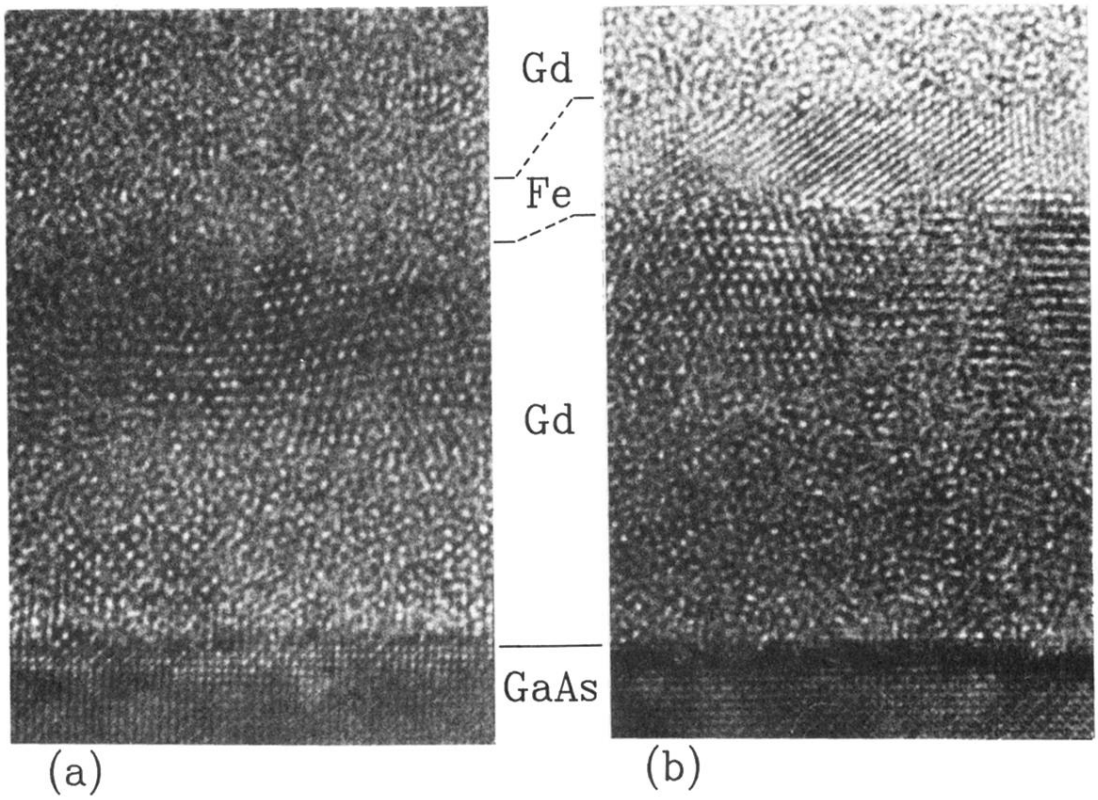

FIG. 4. Cross-section HRTEM images of two GaAs(110)/(10 nm Gd)/Fe/(3 nm Gd)/(10 nm Al) films with thicknesses d_{Fe} of 1.6 nm (a) and 3.2 nm (b). In (b) the Fe interlayer is nanocrystalline.